

Lithium Chloride Therapy Fails to Improve Motor Function in a Transgenic Mouse Model of Machado-Joseph Disease

Sara Duarte-Silva ^{1,2}

Andreia Neves-Carvalho ^{1,2}

Carina Soares-Cunha ^{1,2}

Andreia Teixeira-Castro ^{1,2}

Pedro Oliveira ³

Anabela Silva-Fernandes ^{1,2}

Patrícia Maciel ^{1,2,*}

Phone 351-253-604824

Email pmaciel@ecsaude.uminho.pt

¹ Life and Health Sciences Research Institute (ICVS), School of Health Sciences, University of Minho, Campus Gualtar, 4710-057 Braga, Portugal

² ICVS/3B's - PT Government Associate Laboratory, Braga/Guimarães, Portugal

³ ICBAS - Abel Salazar Biomedical Sciences Institute, University of Porto, Porto, Portugal

AQ1

Abstract

The accumulation of misfolded proteins in neurons, leading to the formation of cytoplasmic and nuclear aggregates, is a common theme in age-related neurodegenerative diseases, possibly due to disturbances of the proteostasis and insufficient activity of cellular protein clearance pathways. Lithium is a well-known autophagy inducer that exerts neuroprotective

effects in different conditions and has been proposed as a promising therapeutic agent for several neurodegenerative diseases. We tested the efficacy of chronic lithium (10.4 mg/kg) treatment in a transgenic mouse model of Machado-Joseph disease, an inherited neurodegenerative disease, caused by an expansion of a polyglutamine tract within the protein ataxin-3. A battery of behavioral tests was used to assess disease progression. In spite of activating autophagy, as suggested by the increased levels of Beclin-1, Atg7, and LC3-II, and a reduction in the p62 protein levels, lithium administration showed no overall beneficial effects in this model concerning motor performance, showing a positive impact only in the reduction of tremors at 24 weeks of age. Our results do not support lithium chronic treatment as a promising strategy for the treatment of Machado-Joseph disease (MJD).

AQ2

Keywords

Polyglutamine
Spinocerebellar ataxia
Lithium
Autophagy
Therapy
Triplet repeats

Electronic supplementary material

The online version of this article (doi: 10.1007/s12311-014-0589-9) contains supplementary material, which is available to authorized users.

Introduction

Lithium, a monovalent cation and a FDA-approved drug with the ability to cross the blood–brain barrier, has been used in the past 6 decades for the treatment of bipolar disorder (BD) and also adjunctively with mood stabilizers and antidepressants to enhance, prolong, and facilitate treatment response and remission of mood disorders [1, 2]. Although its therapeutic mechanisms remain unclear, strong in vivo and in vitro evidence suggests that lithium has neurotrophic/neuroprotective properties toward a wide range of insults, and also in neurodegenerative diseases [3, 4]. Lithium inhibits glycogen synthase kinase-3 [5, 6] and increases the protein levels of the brain-derived

neurotrophic factor (BDNF) [7, 8], leading to an enhanced cell survival. Lithium also regulates calcium homeostasis and suppresses calcium-dependent activation of pro-apoptotic signaling pathways [9], and it can protect against endoplasmic reticulum (ER) stress [10], associated with impaired synaptic plasticity and pathology in neurodegenerative conditions, such as Alzheimer's disease (AD) [11]. In order to be effective, lithium requires long-term treatment, and its effects are not reverted immediately after discontinuation. For this reason, it is thought that lithium acts at the gene expression level. Indeed, lithium is able to upregulate the expression of important molecules such as HSP70 [12, 13], BCL-2 [9, 14, 15], BDNF [7, 8, 16], HSF1 [13], and CREB [4], among others. Moreover, lithium decreases inositol 1,4,5-trisphosphate by inhibiting phosphoinositol phosphatases [17, 18]; this was proposed as a novel mechanism to induce autophagy [19–21]. Macroautophagy, commonly referred to as autophagy, is an important process for the degradation of proteins and organelles and plays a major role in cellular stress conditions [22]. It is also involved in neuronal and astrocytic cell survival and function [23]. The process of autophagy begins with the formation of double-membrane structures called autophagosomes that fuse with lysosomes (autolysosomes) and later degrade their contents by lysosomal hydrolytic enzymes [24, 25]. Autophagy recycles cytoplasmic proteins in normal conditions and recycles nutrients when necessary, for instance, under starvation. The accumulation of misfolded proteins in cells is a common feature in aging and in several neurodegenerative disorders [26], which makes autophagy a prominent target for the treatment of such diseases; these include amyotrophic lateral sclerosis (ALS), Parkinson disease (PD), AD, Huntington's disease (HD), and Machado-Joseph disease (MJD) [27–37]. Drugs that potentially modulate autophagy are increasingly being used in clinical trials, and screens are being performed for the discovery of new compounds that induce autophagy. Autophagy is modulated by several signaling pathways and is directly inhibited by the serine/threonine protein kinase mammalian target of rapamycin (mTOR) [38]. Administration of rapamycin has been demonstrated to be beneficial in different animal models of neurodegenerative disorders, by enhancing autophagic function [24, 29, 36, 39, 40]. Autophagy can also be regulated independently of mTOR, which can be achieved through lithium, sodium valproate, and carbamazepine, compounds that lower myo-inositol-1,4,5-triphosphate levels [20, 41]. Lithium acts as an autophagy enhancer or inhibitor, depending on the dosage. At higher doses, it inhibits GSK3 β , which suppresses autophagy [42]; in contrast, at lower doses, it inhibits IMPase,

inducing autophagy [20].

Chronic lithium treatment was tested in several models of neurodegenerative diseases. Lithium was shown to have beneficial effects in patients and also in an ALS mouse model [43, 44]. The study in the mouse model demonstrated neuroprotection by lithium, which delayed disease onset and duration and increased lifespan. In the clinical trial, a randomized study of adults with ALS showed that none of the patients treated with lithium died during the 15 months of the follow-up, and the disease progression was markedly attenuated [44]. In a mouse model of HD, this treatment had variable effects; lithium improved the motor performance and reduced depressive-like behavior, but only when administered post-symptomatically [45]; furthermore, it had no effect on survival in this model [45]. Chronic treatment with lithium also improved neurological function and hippocampal dendritic arborization in a mouse model of SCA1 [46]. More recently, chronic lithium treatment was shown to ameliorate the phenotype of a MJD *Drosophila* model, partially by inhibiting GSK3 β [47].

Taking into account the beneficial effects of lithium and its autophagy induction properties, and considering that little is known about its possible effects in MJD, we performed chronic lithium treatment in the CMVMJD135 mouse model [48]. Our results show limited beneficial effects of lithium treatment; although it subtly improved a few of the symptoms observed at specific time points, it was not able to globally improve motor function in this model. These findings do not support the idea that lithium is a good candidate to treat MJD. This is of clinical relevance, since one may avoid the collateral effects of trying lithium therapy in MJD patients.

Material and Methods

Transgenic Mice

We used the CMVMJD135 mice [48], which express an expanded version of the human MJD1-1 cDNA (the 3 UIMs-containing variant of ATXN3) under the regulation of the CMV promoter (ubiquitous expression) at near-endogenous levels. All animals were maintained under standard laboratory conditions: an artificial 12-h light/dark cycle (lights on from 8:00 to 20:00 h), with an ambient temperature of 21 ± 1 °C and a relative humidity of 50–60 %; the mice were given a standard diet (4RF25 during the gestation and postnatal periods, and 4RF21 after weaning, Mucedola SRL, Settimo

Milanese, Italy) and water ad libitum. All procedures were conducted in accordance with European regulations (European Union Directive 86/609/EEC). Animal facilities and the people directly involved in animal experiments (S.D.S, A.N.C) were certified by the Portuguese regulatory entity—Direcção Geral de Veterinária. All of the protocols performed were approved by the joint Animal Ethics Committee of the Life and Health Sciences Research Institute, University of Minho. Health monitoring was performed according to FELASA guidelines [49], confirming the Specified Pathogen Free health status of sentinel animals maintained in the same animal room. Humane endpoints for experiment were defined (20 % reduction of the body weight, inability to reach food and water, presence of wounds in the body, dehydration), but not needed as the study period was conceived to include ages at which animals do not reach these endpoints.

Mouse Genotyping

The progenies produced by mating MJD transgenic with wild-type animals were genotyped at weaning by PCR, as previously described [50].

Drug Treatment and Behavioral Tests

Male mice were used in the study since they show less variability than females in behavioral tests, due to the more variable hormonal female status. Transgenic and non-transgenic, drug- and vehicle-treated animals were housed at weaning in groups of five animals per cage. The experiment started at 4 weeks and ended at 24 weeks of age. At 4 weeks of age, we screened the overall status of the animals by the SHIRPA protocol before starting the treatment with lithium chloride (LiCl, Merck, Massachusetts, USA). The treatment started at the asymptomatic age of 5 weeks, 1 week before the previously observed onset of symptoms [48].

We used a total of 40 animals, which were housed according to the drug administered, since the experiment was carried out by a single experimenter, which was only blind to the genetic status of the animals. The animals were intraperitoneally injected three times per week, except in the week of behavioral tests. Transgenic and non-transgenic littermates ($n = 10$ for each genotype) were treated with 10.4 mg/kg of lithium chloride as previously described [44, 45]. Control littermate animals were given a vehicle injection of buffer (0.15 M NaCl, 5 % Tween-20, and 5 % PEG 400) with the same frequency. The animals were evaluated at 20 and 24 weeks of age in the Beam Walk Balance test. The SHIRPA protocol was performed at all ages tested. For

a detailed description of behavioral testing, see below.

Body Weight

All mice were weighed a week before the start of the drug treatment (4 weeks) and then at 5, 6, 8, 9, 10, 12, 13, 14, 16, 17, 18, and 20 weeks of age.

Beam Walk Balance Test

The beam walk balance test assesses balance but is also sensitive to fine motor coordination. This test measures the ability of the animal to stay upright and to walk on an elevated beam without falling to the cushioned pads below, or slipping to one side of the beam. The beams are 70 cm long and made of smooth wood with a square (12 mm wide) or a round (11- and 17-mm diameter) shape. The beam is placed at the height of 50 cm. The test has different levels of difficulty obtained by varying the shape and width of the beams. The animals were trained during 3 days in the square beam (12 mm). In the fourth day, they were tested in the training beam and also in two round beams (17 and 11 mm).

The animal is placed on one end of the beam and then allowed to walk along the beam and reach the opposite end (which has a “safe” dark box). At the end of the training days, the animals should be capable of performing the task in less than 20 s. By day 4, animals were tested using two beams of different width and shape (square and round). If the animal fell or turned around in the beam, this was considered one failed trial. Each animal had the opportunity to fail two times in each beam. The time the animal took to cross the beam was counted, and time was discounted if the animal stopped in the beam.

SHIRPA Protocol

We established a protocol for phenotypic assessment based on the primary screen of the SHIRPA protocol, which mimics the diagnostic process of general neurological and psychiatric examination in humans [51]. Each mouse was placed in a viewing jar (15-cm diameter) for 5 min and transferred to a 15-labeled-squares arena (55 × 33 × 18 cm), and then a series of anatomical and behavioral features were registered. The full details of the SHIRPA protocol are available at the site http://empress.har.mrc.ac.uk/browser/?sop_id=10_002_0. In addition, we included the footprint pattern test (see below) to assess gait [52] and the counting of rears over 5 min in the viewing jar, as a measure of spontaneous vertical exploratory activity. The protocol was adjusted in order to minimize animal handling and to generate

uniformity in waiting times between the tests [53].

Footprint Pattern

The footprint test was used to evaluate the foot dragging of the animals. To obtain footprints, the hindpaws and forepaws of the mice were coated with black and red non-toxic paints, respectively. A clean rectangular paper sheet was placed on the floor of the runway for each run. The animals were then allowed to walk along a 100 cm long \times 4.2 cm width \times 10 cm height corridor in the direction of an enclosed black box. Each animal was allowed to achieve one valid trial per age. To evaluate the presence of foot dragging through age, the footprinting pattern of CMVMJD135 and wild-type (wt) vehicle- and lithium-treated ($n = 10$ per group) was analyzed at each time point considering six consecutive steps (absent, no dragging; present, at least one step out of six shows dragging).

AQ3

Assessment of Autophagy Activation

The animals that were chronically treated with LiCl for 19 weeks and were killed 12 h after the last injection as previously described [48], and the brain and muscle tissue were immediately frozen in dry ice. We also injected wild-type animals with LiCl (10.4 mg/kg) three times in 1 week in alternate days and performed the killing at different time points after the last injection: 6, 14, 16, 18, and 24 h for determination of acute effects. Another set of animals was injected with the vehicle and killed at the same time points.

AQ4

Western Blot

Brain tissue was homogenized in cold 0.1 M Tris-HCl, pH 7.5, 0.1 M EDTA, and a mixture of protease inhibitors (Complete, Roche, Swiss) and was sonicated for 10 s. Protein concentration was determined using the Bradford assay (Biorad, CA, USA). Samples were heated for 5 min at 100 °C and microfuged for 10 s before loading. For each sample, 15 μ g of total protein was loaded into SDS-PAGE gels and then transferred to nitrocellulose membranes (Amersham GE Healthcare, UK). After incubation with the primary antibodies—rabbit anti-LC3 (1:1,000 Novus Biologicals, Littleton, CO), rabbit anti-IMPA1 (1:1,000, Abcam, Cambridge, UK), rabbit anti-p62 (1:50, Abcam, Cambridge, UK), rabbit anti-Beclin-1 (1:1,000, Cell signaling, Beverly, MA), rabbit anti-Atg7 (1:1000, Cell signaling, Beverly, MA), mouse

anti-alpha-tubulin (1:100, DSHB, University of Iowa, Iowa), and mouse anti-beta-actin (1:100, DSHB, University of Iowa, IA)—the secondary antibodies were incubated at the following dilutions: anti-rabbit (1:10.000, Santa Cruz, Dallas, TX, USA) and anti-mouse (1:10.000, Santa Cruz, Dallas, TX, USA). Antibody affinity was detected by chemiluminescence (ECL kit, Santa Cruz, Dallas, Texas, USA). Band quantification was performed using the ImageJ software according to the manufacturer's instructions, using alpha-tubulin as the loading control.

Determination of Lithium Plasma Levels

The plasma lithium levels were measured applying the LITH assay using the Dimension Vista® System (LITH Flex® reagent cartridge)—SIEMENS.

Statistical Analysis

Power analysis was used to determine the sample size [54]. Considering the different variables under study, such as weight and time held in the hanging wire, assuming a power of 0.8 and a significance level of 0.05, different required sample sizes were obtained, depending on the specified smallest detectable difference and the variability of the experimental groups. Based on these calculations and bearing in mind that as the age of the animals increases, also the mean differences increase and, possibly, the standard deviations, a sample size ranging between five and ten animals was obtained, and therefore, a sample of ten animals was chosen. For specific behavioral tests and time points of analysis, see Supplementary Table S1.

Continuous variables with normal distributions (K-S test $p > 0.05$) were analyzed with the Student's t test or two-way ANOVA (factors: genotype and treatment). Behavioral data were subjected to the non-parametric Mann–Whitney U test when variables were non-continuous or when a continuous variable did not present a normal distribution (Kolmogorov-Smirnov test $p < 0.05$). Categorical variables in the SHIRPA protocol were analyzed by contingency tables (Fisher's exact test). All statistical analyses were performed using SPSS 22.0 (SPSS Inc., Chicago, IL). A critical value for significance of $p < 0.05$ was used throughout the study.

Results

In the CMVMJD135 transgenic mouse model, mutant ataxin-3 expression is close to the endogenous levels and the MJD-like symptoms are progressive in

life, as observed in human patients [48]. In the current study, we confirmed the onset of the neurological phenotype at 6 weeks of age, with loss of grip strength, measured using the hanging wire test. At 20 weeks of age, the animals showed a deficit in balance on the beam test. It was also possible to observe tremors, foot dragging, and limb claspings. Furthermore, they exhibited decreased locomotor and exploratory behavior late in life. This model does not show premature death, allowing long-treatment periods—in the present case, treatment was administered for 19 weeks, i.e., until the age of 24 weeks, when animals display overt symptoms and a full-blown neurological phenotype.

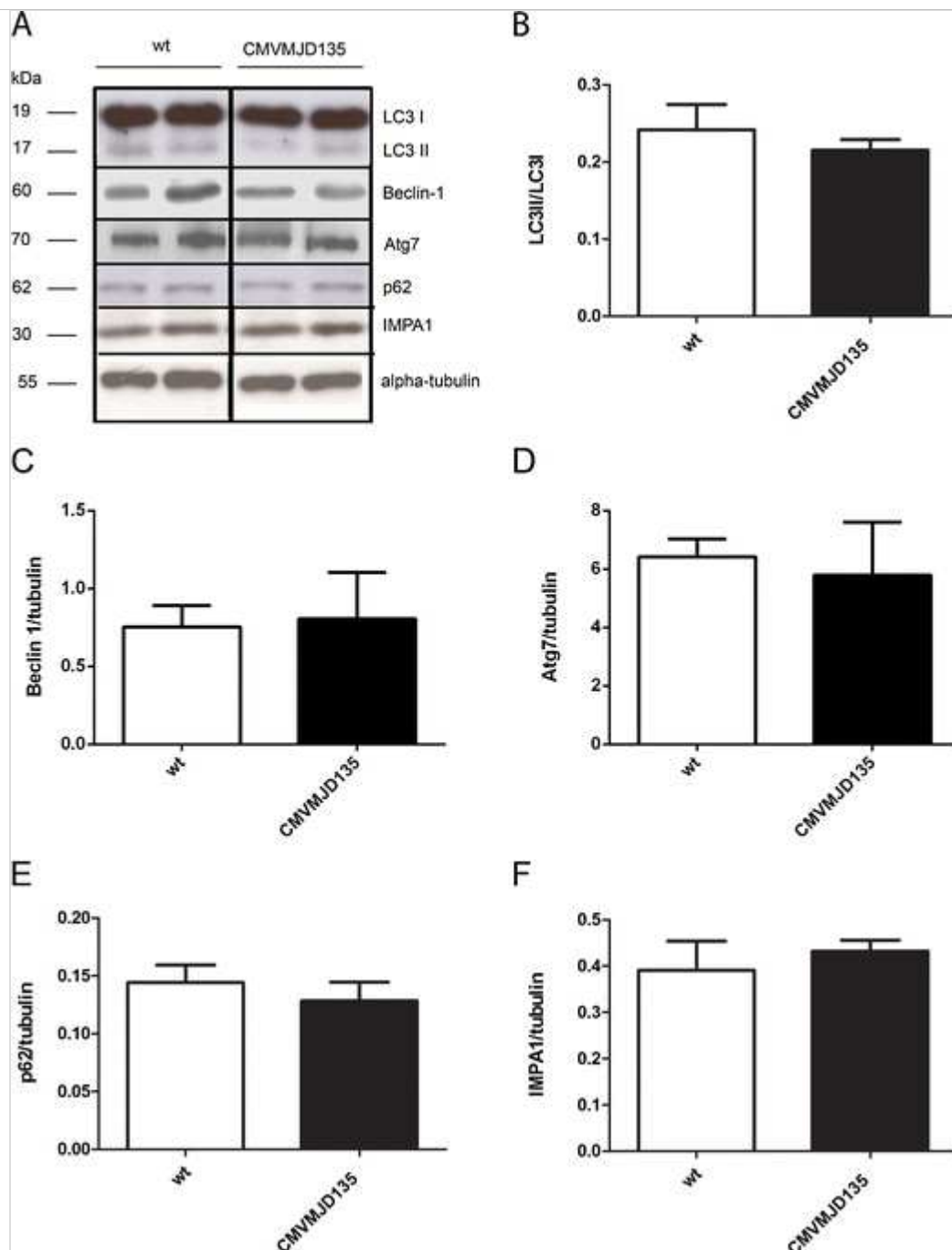
Autophagy Is not Altered in the Brain of CMVMJD135 Mice

At basal conditions, autophagic activity in 24-month-old CMVMJD135 mouse brains did not differ from that of littermate controls (Fig. 1a). Autophagy was assessed by the measurement of protein levels of LC3-II (Fig. 1b), an autophagosome marker; of Beclin-1 (Fig. 1c), a protein involved in the nucleation step of autophagy; of Atg7 (Fig. 1d) involved in the elongation step of this process; of p62 (Fig. 1e), an autophagy substrate; and of IMPA1 (Fig. 1f), an enzyme responsible for the provision of inositol required for synthesis of phosphatidylinositol and polyphosphoinositides. Our results suggest that autophagy is neither impaired nor over-activated in this transgenic mouse model of MJD.

Fig. 1

Autophagy basal levels in CMVMJD135 mice. **a** Representative Western blot probed with LC3, Beclin-1, Atg7, p62, IMPA1, and tubulin antibodies. At least three technical replicates were performed. **b–f** LC3-II, Beclin-1, Atg7, p62, and IMPA1 protein levels were measured in brain lysates of CMVMJD135 mice ($n = 5$) and their littermate wild type ($n = 5$) at 24 months of age. LC3-II protein levels were normalized both for LC3-I and α -tubulin; Beclin-1, Atg7, p62, and IMPA1 were normalized for α -tubulin. * $p < 0.05$; ** $p < 0.01$; *** $p < 0.001$ (Student's t test)

AQ5



Lithium Chloride Induces Autophagy in the Mouse Brain

In order to verify if lithium chloride could induce autophagy at the dosage we planned to administer (10.4 mg/kg), similar to that used by Fornai et al. [44 and Wood and Morton 45], we used a group of wild-type mice, injected them with lithium chloride [45] three times per week, and measured the levels of autophagy markers in the brain at different time points after the last injection (6, 14, 16, 18, and 24 h post-injection). In these mice, in which the mean plasma lithium concentration achieved was 0.3 ± 0.09 mmol/L, we were able to observe an increase in the LC3-II/LC3-I ratio (Fig. 2a) and a decrease in IMPA1 (Fig. 2b), an enzyme whose expression is directly inhibited by lithium. According to the *Guidelines for the use and interpretation of assays*

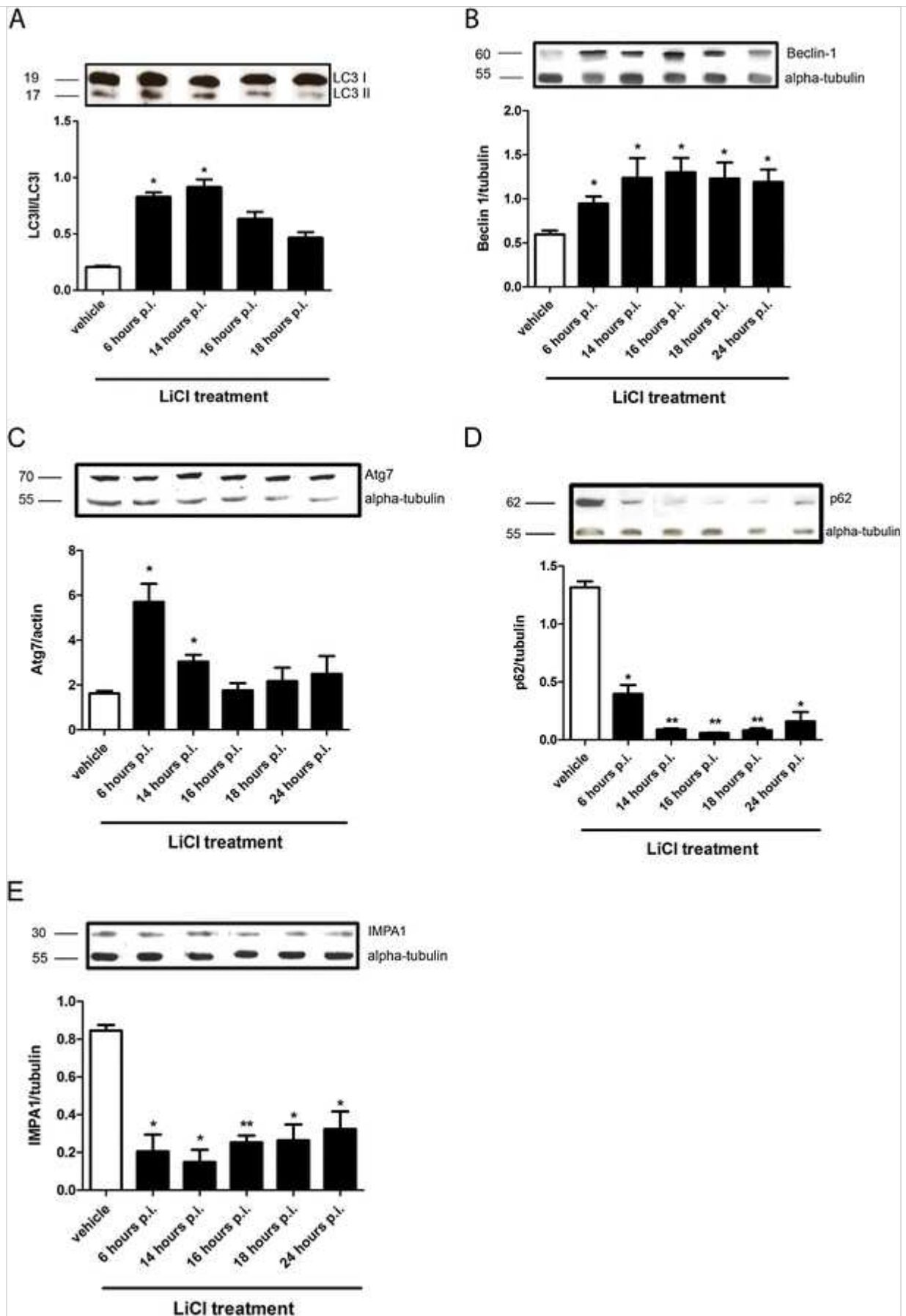
for monitoring autophagy in higher eukaryotes [55], LC3 is the only marker for autophagosomes, but in mammalian cells, total LC3 protein levels may not be altered after a cellular challenge; the most probable finding is the increase in the conversion of LC3-I to LC3-II. LC3-I is abundant and stable in the central nervous system, which is a parameter to take in consideration in this type of measurements [55]. Importantly, the LC3-II/LC3-I ratio was increased at the protein level in the brain of lithium-treated mice (Fig. 2a). We also found an increase in LC3-II/LC3-I ratio in muscle tissue (data not shown). Consistently, Beclin-1, a protein involved in the nucleation step of the autophagosome formation [56], was also increased in animals treated with LiCl, supporting autophagy induction by this treatment (Fig. 2b). Furthermore, the levels of Atg7, a protein involved in the elongation step of autophagosome formation, were also increased in the LiCl-treated animals (Fig. 2c). The decrease in p62 levels confirms that autophagy was occurring without blockage (Fig. 2d). The levels of IMPA1 were, as expected, decreased (Fig. 2e).

Fig. 2

Autophagy induction by acute lithium treatment. **a** Anti-LC3 Western blot of brain lysates of wild-type animals injected with vehicle ($n=4$) or lithium 10.4 mg/kg ($n=4$ for each time point); **b** Beclin-1 Western blot of brain lysates of wild-type animals injected with vehicle ($n=4$) or lithium 10.4 mg/kg ($n=4$ for each time point); **c** Atg7 Western blot of brain lysates of wild-type animals injected with vehicle ($n=4$) or lithium 10.4 mg/kg ($n=4$ for each time point); **d** p62 Western blot of brain lysates of wild-type animals injected with vehicle ($n=4$) or lithium 10.4 mg/kg ($n=4$ for each time point); **e** anti-IMPA1 Western blot analysis of brain lysates of wild-type animals injected with vehicle ($n=4$) or lithium 10.4 mg/kg ($n=4$ for each time point); lithium-injected animals were killed at different time points as shown in the *graph*; vehicle animals were killed 6 h post-injection. Alpha-tubulin or beta-actin was used as loading control. * $n p < 0.05$; ** $n p < 0.01$; *** $n < 0.001$ (Student's *t* test)

AQ6

AQ7



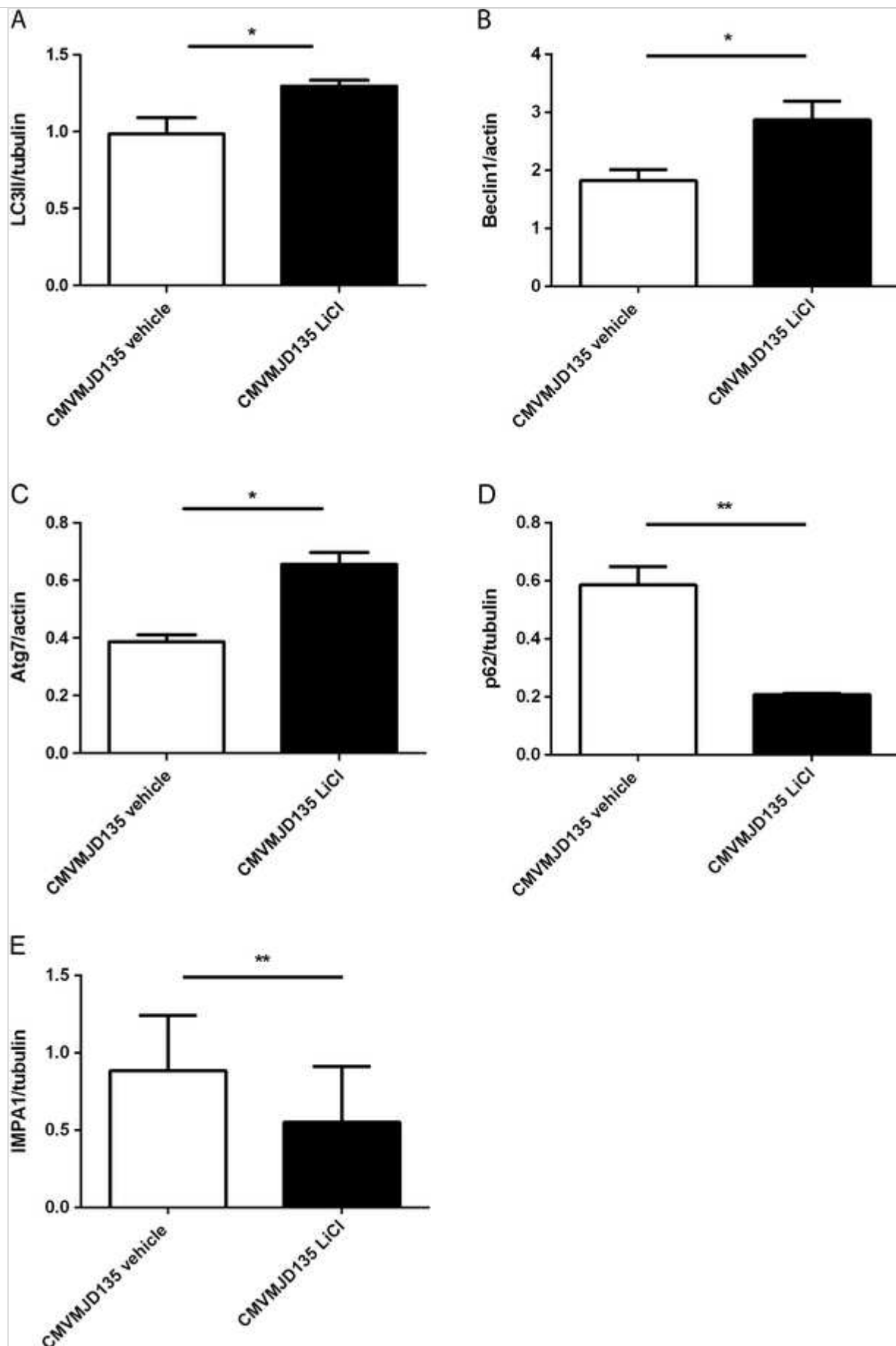
To complement these analyses, we measured the levels of autophagy markers in the brain of the transgenic animals that were chronically treated with LiCl, namely, the LC3-II/LC3-I ratio (Fig. 3a), as well as protein levels of Beclin-1

(Fig. 3b), Atg7 (Fig. 3c), p62 (Fig. 3d), and IMPA1 (Fig. 3e), and the results were similar to those observed for the acute LiCl treatment, confirming that autophagy remains induced in the chronically treated animals.

Fig. 3

Autophagy induction by lithium in chronically treated transgenic mice at 24 weeks of age. **a** Anti-LC3 Western blot of brain lysates of transgenic animals injected with vehicle ($n = 4$) or lithium 10.4 mg/kg ($n = 4$); **b** Beclin-1 Western blot of brain lysates of transgenic animals injected with vehicle ($n = 4$) or lithium 10.4 mg/kg ($n = 4$); **c** Atg7 Western blot of brain lysates of transgenic animals injected with vehicle ($n = 4$) or lithium 10.4 mg/kg ($n = 4$); **d** p62 Western blot of brain lysates of transgenic animals injected with vehicle ($n = 4$) or lithium 10.4 mg/kg ($n = 4$); **e** anti-IMPA1 Western blot analysis of brain lysates of transgenic animals injected with vehicle ($n = 4$) or lithium 10.4 mg/kg ($n = 4$); alpha-tubulin or beta-actin was used as loading control. $*p < 0.05$; $**p < 0.01$; $***p < 0.001$ (Student's t test)

AQ8



Intriguingly, and despite the efficacy of LiCl to induce autophagy, it did not reduce the protein levels of mutant human ataxin-3 in the brain of LiCl-treated

animals, which were comparable to those of vehicle-treated mice (Supplementary Fig. S1).

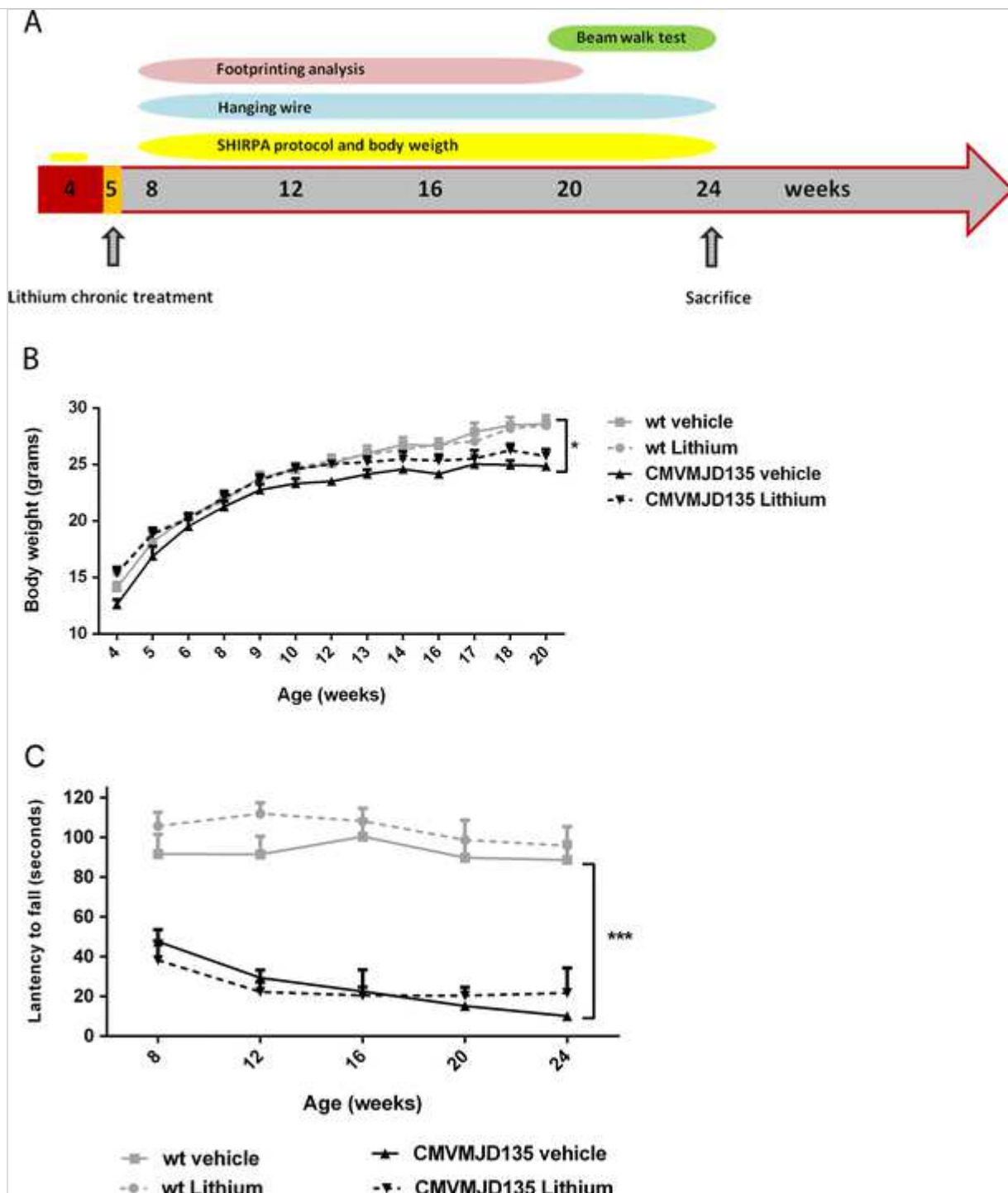
Lithium Did not Improve Body Weight Loss in CMVMJD135 Mice

We assessed the phenotype of the mice from 4 to 24 weeks of age (Fig. 4a). Animals were weighed at 4 (before the treatment) 5, 6, 8, 9, 10, 12, 13, 14, 16, 17, 18, and 20 weeks of age. One of the known collateral effects of lithium treatment in human patients is weight gain [57], but we did not observe this in our study. Chronic administration of LiCl had no effect on body weight in wt animals, compared with wt animals treated with vehicle. At 12 weeks of age, vehicle-treated CMVMJD135 mice started to lose weight compared to the vehicle-treated wt animals ($p = 0.024$) as previously observed for this model [48] (genotype: $F_{1,40} = 9.919$; $p = 0.003$) and as it is known to occur in human patients [58]; this body weight reduction was progressive in time, as shown in Fig. 4b. No differences were found between vehicle- and lithium-treated transgenic animals, i.e., lithium treatment did not improve this body weight reduction.

Fig. 4

Effect of lithium treatment on body weight and strength of CMVMJD135 and wt mice. **a** Schematic timeline for the behavioral analysis of lithium pre-clinical trial. **b** The body weight in grams between 8 and 20 weeks of age was depicted for wt and CMVMJD135 mice treated with LiCl or vehicle ($n = 10$ for each group). **c** Hanging wire test—all transgenic animals display a worse performance in holding the grid with age (from 8 to 24 weeks of age). A maximum time of 2 min was given to each animal and the time that they took to fall was registered ($n = 10$ for each group). Symbols represent mean \pm SEM of the different groups. * $p < 0.05$; ** $p < 0.01$; *** $p < 0.001$, for genotype factor (two-way ANOVA)

AQ9



Lithium Treatment Had no Major Effect on Neurological Deficits Present in CMVMJD135 Mice

We analyzed all the animals using the SHIRPA protocol [51] before the treatment onset, at 4 weeks of age, and no differences were found between wt and CMVMJD135 animals (data not shown), meaning that at this time point, the transgenic animals did not show any symptoms of disease.

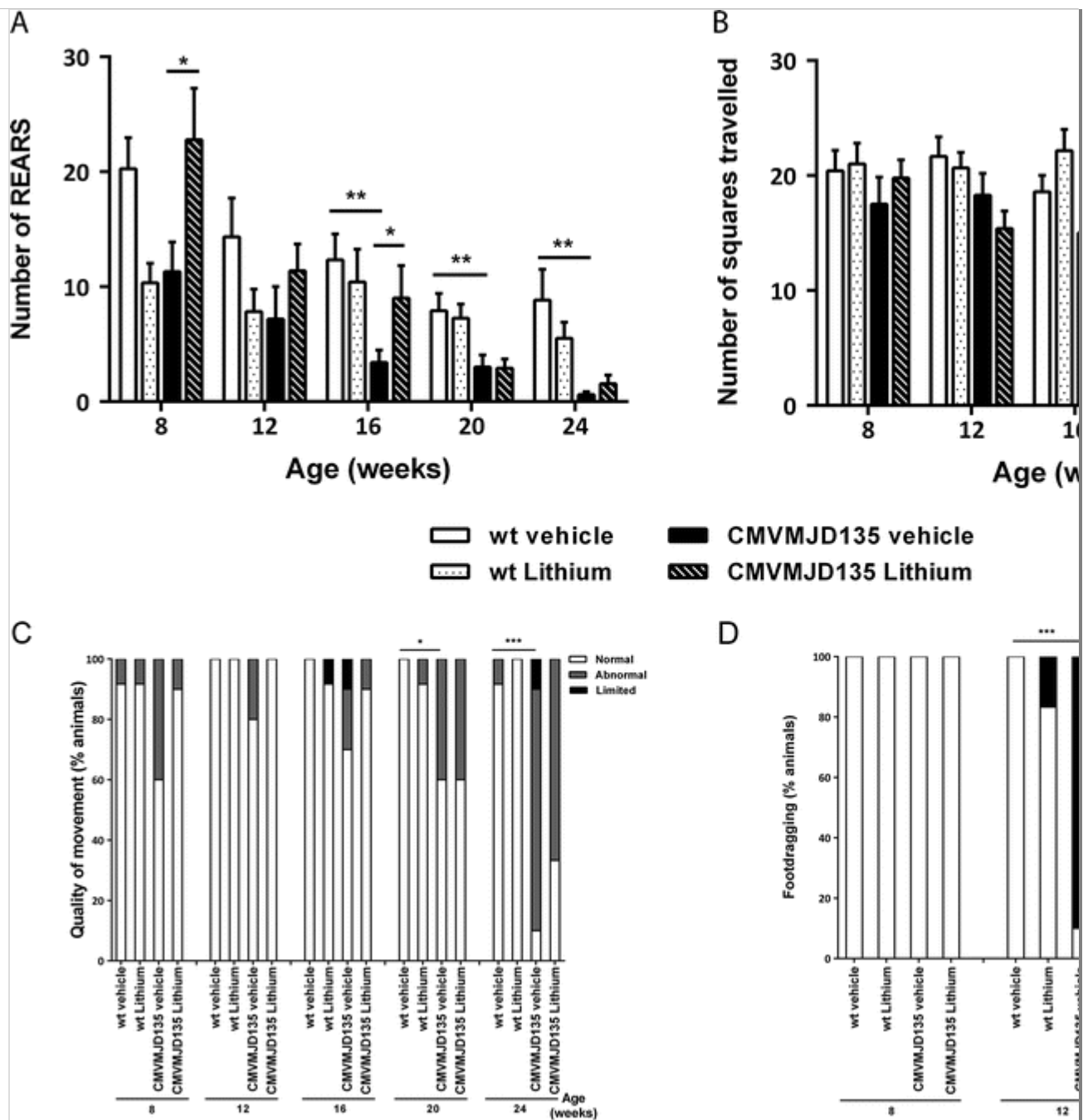
The first disease manifestation in the CMVMJD135 model is the loss of limb strength given by the hanging wire test, which measures the time the mouse is able to hold a grid with its hindlimbs and, mostly, forelimbs, before falling.

Whereas wild-type animals—treated and vehicle groups—were almost always able to complete the task (hanging in the grid for the maximum time, 2 min), transgenic animals—both LiCl- and vehicle-treated groups—showed a decreased latency to fall from the grid, worsening with age (genotype: $F_{1,39} = 324.589$; $p = 1.6628 \times 10^{-20}$) (Fig. 4c).

At 16 weeks and subsequent ages, CMVMJD135 vehicle-treated animals showed a decrease in exploratory behavior, given by the infrequent rearing behavior, which progressed to almost no rearing at the age of 24 weeks ($p < 0.05$). At 8 weeks of age, lithium-treated CMVMJD135 animals showed an increase in exploratory behavior when compared with vehicle-treated CMVMJD135 animals, given by the increase in number of rears in the viewing jar ($p = 0.026$). This activity reached that of the vehicle-treated wt animals at this age, but at later stages, the improvement was no longer seen (Fig. 5a). To further test exploratory locomotor activity, we counted the number of squares travelled in the arena used in the SHIRPA protocol. CMVMJD135 treated with vehicle showed a decrease in the number of squares travelled in the arena at 20 and 24 weeks of age ($p = 0.003$ and $p = 0.002$, respectively), which was not improved by chronic lithium treatment (Fig. 5b).

Fig. 5

Effect of lithium treatment upon spontaneous exploratory activity and gait quality. **a** Transgenic animals display decreased vertical locomotor activity at 16 weeks of age and subsequent ages ($n = 10$ for each group); **b** Transgenic animals travel less in the arena than wild-type animals at 20 and 24 weeks of age; lithium treatment had no effect in this phenotype ($n = 10$ for each group). **c** CMVMJD135 animals have abnormal gait at 20 and 24 weeks of age (qualitative assessment) that is slightly reverted by LiCl at 24 weeks, although not statistically significant ($n = 10$ for each group). **d** Quantitative analysis of the foot dragging: Presence/absence of dragging demonstrated that transgenic animals drag their feet since 12 weeks of age, which was not ameliorated by LiCl ($n = 10$ for each group). * $p < 0.05$; ** $p < 0.01$; *** $p < 0.001$



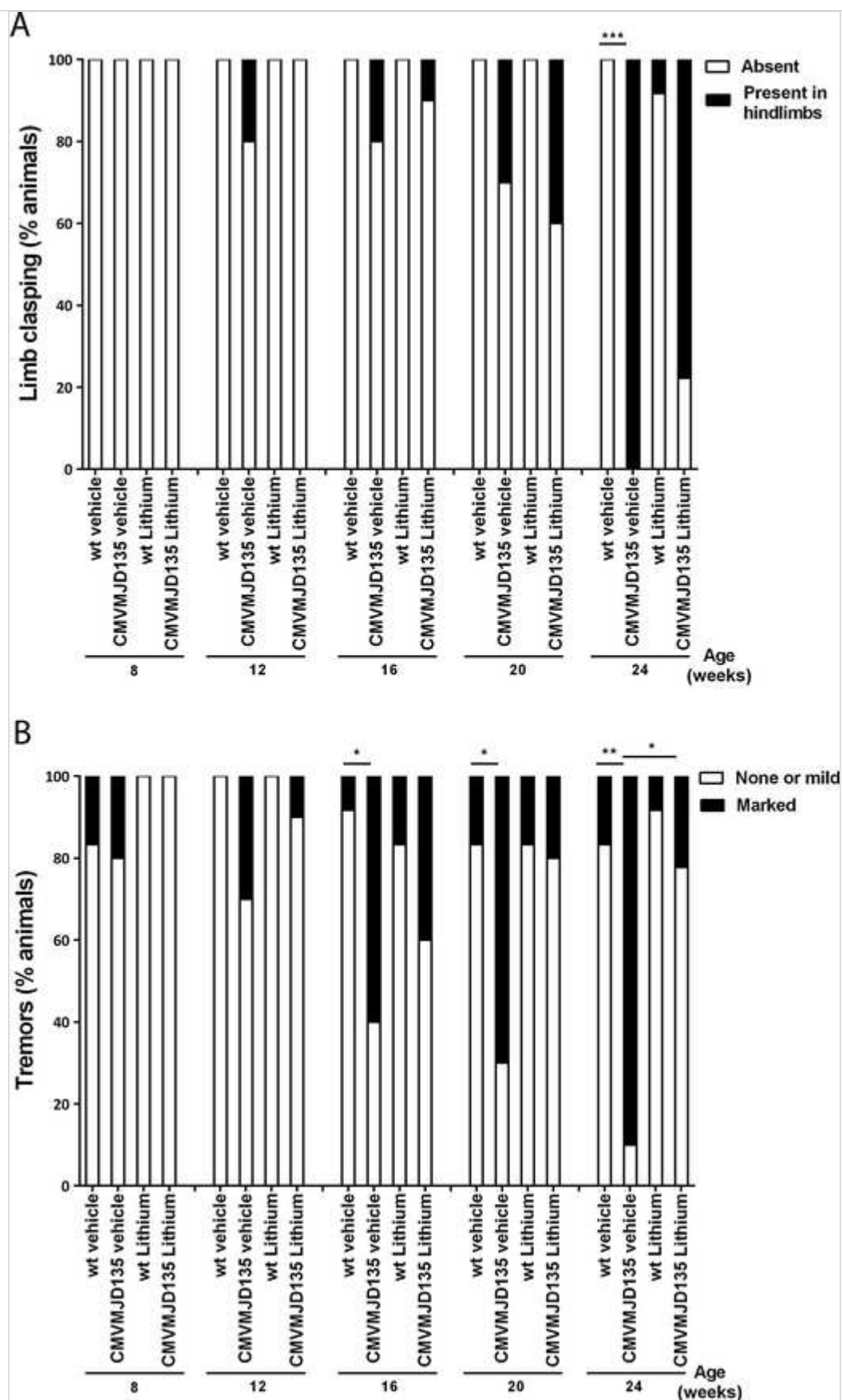
We also performed qualitative analysis of the gait in the open arena as described by Rogers et al. [51]. We scored the animals with 0 when their gait was normal, 1 when the animal had a fluid stepping but an abnormal walking, and 2 when the animal had limited walking [51]. CMVMJD135 animals started to have significantly worse gait scores at the age of 20 weeks ($p = 0.029$), and at 24 weeks of age, 100 % of the animals had a visibly abnormal gait (80 % of the animals were scored as 1, 10 % as 2, and 10 % as 0, $p = 0.000017$) (Fig. 5c). There was a trend toward improvement with lithium treatment, but only at 24 weeks of age (80 % of the vehicle transgenic animals were scored as having abnormal gait, in contrast with 67 % of the treated transgenic animals, $p = 0.054$) (Fig. 5c). Additionally, we performed a semi-quantitative analysis of the foot dragging observed in the mice (Fig. 5d).

We found no significant differences in the footstep measurements between the four groups at the ages tested, but it was possible to observe that CMVMJD135 animals presented foot dragging at 12 weeks ($p = 0.00002$) and that this symptom progressed in severity with age ($p < 0.05$). At 20 weeks of age, all CMVMJD135 mice (100 %, $p = 2 \times 10^{-5}$) dragged their feet while walking. Lithium was not able to rescue this phenotype.

When mice are picked up by the tail and suspended toward a surface, their normal reflex is to extend all the four paws to anticipate the ground [59]. The paw clasp phenotype, in which the animals contract the paws instead of extending them, is observed in several mouse models with damage in the cerebellum [60, 61] or in the basal ganglia [62, 63], and also in models of AD [64–66]. In CMVMJD135 mice, this paw clasp phenotype was detected at 24 weeks of age ($p = 2 \times 10^{-6}$), whereas wt animals never presented this abnormal reflex (Fig. 6a). Lithium treatment was not able to rescue this aspect of the phenotype (Fig. 6a).

Fig. 6

Effect of lithium treatment on limb clasp and tremors. **a** Limb clasp is observed in transgenic animals—treated and non-treated—at 24 weeks of age ($n = 10$ for each group). **b** CMVMJD135 mice presented tremors since 16 weeks of age; LiCl is able to decrease tremors in transgenic animals at 24 weeks of age ($n = 10$ for each group). * $p < 0.05$; ** $p < 0.01$; *** $p < 0.001$ (Fisher's exact test)



We also observed an increase in the percentage of transgenic animals presenting tremors through age, starting at 16 weeks of age ($p < 0.05$), which was, surprisingly, ameliorated with lithium treatment, this improvement being significant only after a long period of administration (24 weeks of age, $p =$

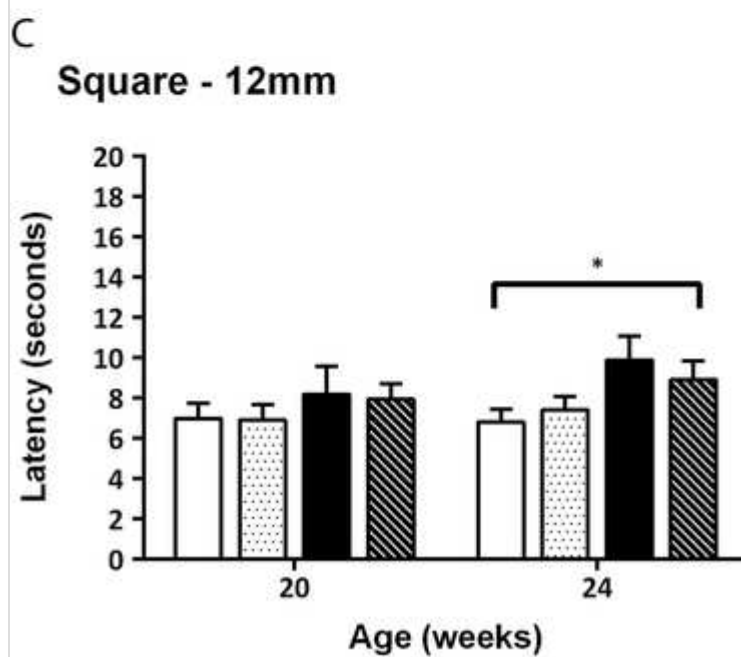
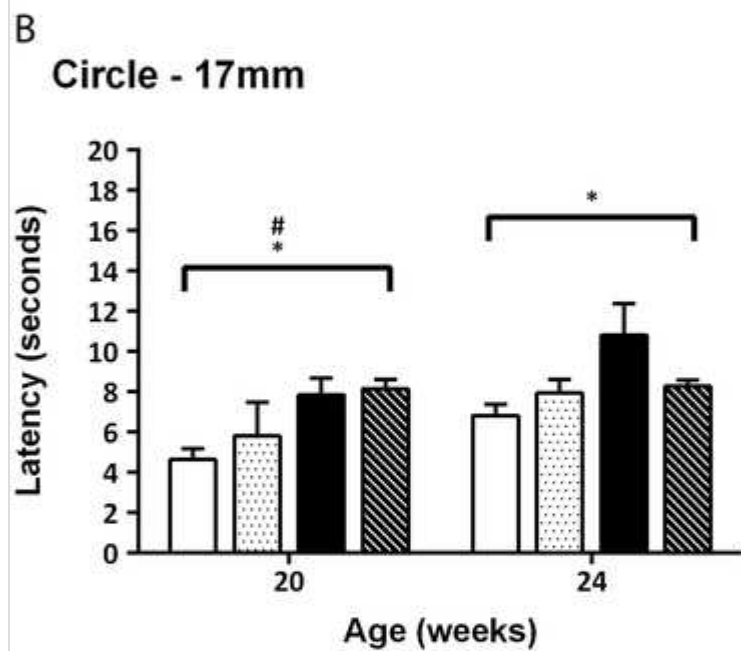
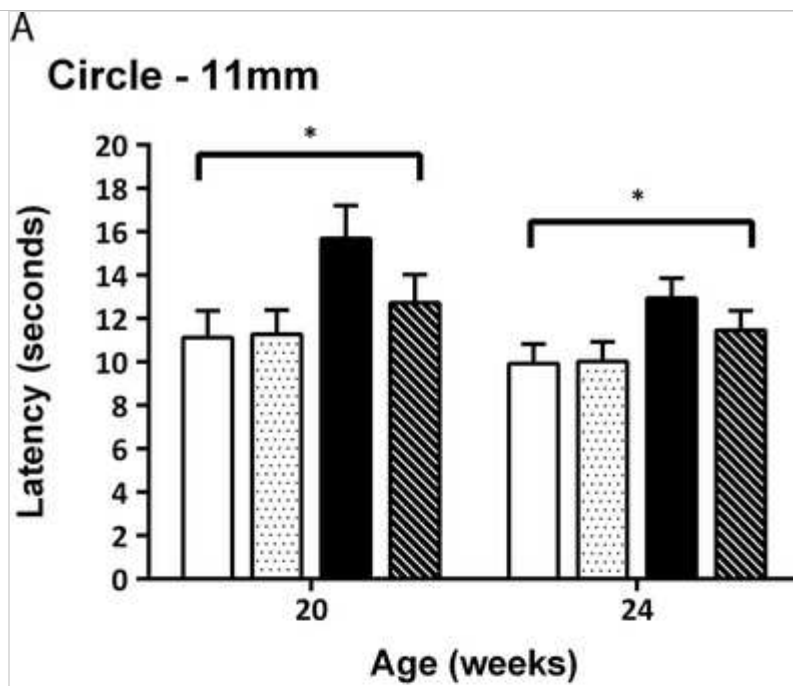
0.02) (Fig. 6b).

Lithium Fails to Rescue Balance and Fine Motor Deficits in CMVMJD135 Mice

The balance beam test depends on the mouse's ability to maintain balance while traversing a narrow beam to reach a safe platform [67] and was used to test the balance and fine motor coordination capabilities in CMVMJD135 and wt animals, treated with LiCl or with the vehicle. At 20 weeks, CMVMJD135 animals were slower to traverse the round beams with 17 mm (genotype: $F_{1,31} = 8.96$; $p = 0.005$; genotype \times treatment: $F_{1,31} = 5.260$; $p = 0.029$) and 11 mm of diameter (genotype: $F_{1,36} = 4.447$; $p = 0.042$), but not significantly slower in the 12-mm square beam, in which they had been trained; the difficulty in performing this task was confirmed at 24 weeks of age, when transgenic animals were slower in traversing the 12-mm square beam (genotype: $F_{1,37} = 6.412$; $p = 0.016$), the 17-mm round beam ($F_{1,30} = 5.315$; $p = 0.028$), and the 11-mm round beam (genotype: $F_{1,33} = 5.041$; $p = 0.032$) (Fig. 7). In the 11-mm round beam, transgenic mice showed a "crawling behavior" (when the animal's thorax and abdomen are in contact with the beam surface) and dragged themselves across the beam. Lithium had no significant effects in the performance in the beam of either wt or CMVMJD135 mice.

Fig. 7

Effect of lithium treatment on balance and motor coordination. Each *bar* corresponds to the mean of two consecutive trials in each beam. The time to traverse the beam was videotaped and then measured by the same experimenter. Ten to 12 animals were used for each condition. * $p < 0.05$ for genotype factor (two-way ANOVA); # $p < 0.05$ for genotype \times treatment factor (two-way ANOVA)



Discussion

One promising therapeutic strategy in diseases associated with misfolded protein accumulation is the stimulation of cellular degradation pathways such as macroautophagy. Here we have tested the effect of autophagy activation by lithium in a mouse model of MJD, beginning at a pre-symptomatic age.

In this study, we confirmed the progressive neurologic phenotype of the CMVMJD135 mouse model, through observation of the group of vehicle-treated animals, which behaved as previously described [48]. Chronic lithium treatment was, however, not able to rescue the neurological phenotype of these mice. The disease-causing polyQ CAG repeat expansion in ataxin-3 might cause neurotoxicity both through a toxic gain of function and a loss of the wild-type ataxin-3 normal function(s) [68]. Several molecular pathways might be involved in MJD neuropathology, although the precise pathogenic mechanism(s) is (are) not known [69, 70]. Decreased autophagy is a cellular process that might be included in these mechanisms [36, 37, 71]. An autophagy impairment was recently proposed to occur in a mouse model of MJD, as well as in the brain of MJD patients [37]. MJD pathogenesis has been modeled through the expression of mutant ataxin-3 that causes aggregate formation and toxicity, in cell models and in vivo [72], and autophagy has been shown to be an effective cellular strategy for the clearance of these aggregated proteins [73, 74]. Menzies and colleagues demonstrated that autophagy induction by rapamycin could improve rotarod performance in a transgenic mouse model of MJD [36]; however, the MJD model used in this study presented a very mild phenotype (not significantly different from control mice from a statistical standpoint), and the authors proposed that this hypothesis should be further confirmed in a model with more marked phenotype. Also, in this study, the authors suggest that it would be of great importance to test other compounds that can induce autophagy, such as lithium. Here, we provide a complete behavioral analysis of the CMVMJD135 mouse model chronically treated with lithium chloride.

At basal conditions, it was not possible to observe significant differences in protein levels of LC3-II, Beclin-1, Atg7, p62, and IMPA autophagy markers when comparing CMVMJD135 with wild-type animals at 24 weeks of age (when they have a well-established phenotype), suggesting that, in spite of the neurodegenerative changes they show [48], the autophagy process is functioning normally in the brain of these mice. This is in contrast with the

findings in another transgenic mouse model of MJD, characterized by more marked overexpression of ataxin-3 and a faster disease progression [75], where it has been proposed that autophagy was over-activated but functional only at early stages of the disease [37].

Given the previous results in other related neurodegenerative diseases and our own results with 17-DMAG, which delayed disease progression in the CMVMJD135 mouse and induced autophagy [48], we reasoned that even if autophagy is normal in these mice, it might be useful to boost the cells' capacity to eliminate toxic ataxin-3 aggregates; hence, we proceeded with chronic lithium treatment in the CMVMJD135 mice. In this study we selected to use a dosage at the lower limit of the therapeutic range in order to avoid cerebellar toxicity as much as possible. The efficacy of lithium as an autophagy inducer in the brain was validated by the decrease in protein levels of IMPA-1, induction of Beclin-1 and Atg7 protein levels, increased LC3-II/LC3-I ratio, and decrease in p62 in treated CMVMJD135 mice. Our reason for studying treatment of the CMVMJD135 mice before onset of the symptoms was to have the strongest effect possible in the disease progression and to see if we could prevent or delay the onset of the disease rather than treat it once established, as mechanistically, we anticipated that it would be harder to remove the larger nuclear inclusions than smaller cytoplasmic aggregates. Considering the availability of a genetic test for MJD patients, this early stage treatment design could be feasible for mutation carriers even before they present clinical symptoms.

At the phenotypic level, LiCl treatment did not rescue the loss of body weight observed in CMVMJD135 animals. Progressive weight loss is observed in MJD patients [58], despite a normal appetite [76] and also in HD patients [77]. It has been reported previously that treatment with LiCl pre-symptomatically caused loss of body weight in a HD mouse model, whereas a gain of body weight was observed when LiCl treatment was performed in post-symptomatic animals [45]. We have not observed loss or gain of body weight as result of the treatment here performed, which was initiated 1 week before symptom onset. Intriguingly, at 8 weeks of age, lithium-treated CMVMJD135 animals showed an increase in exploratory behavior when compared with vehicle-treated CMVMJD135 animals, given by the increase in number of rears in the viewing jar. This activity reached the levels of vehicle-treated wt animals. We believe that this apparent (and transient) amelioration might have been due to an improved reaction to the

novelty of the test (i.e., an effect in mood) and not because lithium was having benefic effects at the motor level, since this rescue of hypoactivity was not manifested in other motor parameters and was not maintained through life.

The tremors observed in CMVMJD135 mice were ameliorated with lithium treatment, this improvement being statistically significant only after a long period of lithium administration. This is an intriguing finding because tremors are often observed in BD patients taking lithium for long periods [78], being a side effect of this drug. Additionally, tremors are not a major symptom in MJD patients, but rather a rare manifestation [79–81] that can be treated with levodopa or dopamine agonists [82]. Thus, the tremor rescue by lithium treatment that we observed in CMVMJD135 mice at one of the time points of analysis might not have a major impact in human patients.

Gait analysis was performed using qualitative analysis, given by the “the way animals walk” in the arena—scored by the experimenter, as part of the SHIRPA protocol [51]—and by the footprinting analysis [52], respectively. In the qualitative gait analysis, vehicle-treated CMVMJD135 animals showed visible deficits in gait at 20 and 24 weeks of age. In the last time point of analysis (at 24 weeks), LiCl treatment appeared to improve the visible quality of gait, but this effect was not statistically significant.

Regarding balance (balance beam test), abnormal reflexes (limb claspings), and strength/fine motor coordination (hanging wire test), it was also not possible to observe any amelioration of CMVMJD135 mice with lithium treatment. Of notice, the number of animals used in the study allowed detection of a 50 % effect size for all tests for at least one age, with the exception of the medium square and small circle beams in the balance beam test and the exploratory locomotor activity in the SHIRPA protocol (Supplementary Table S1).

Lithium was shown to have beneficial effects in motor performance (given by rotarod analysis) in a transgenic mouse model of SCA1 [46] but had no effect in motor performance in a HD mouse model when administered pre-symptomatically [45]. The current study demonstrates that long-term peri-symptomatically initiated lithium treatment had no major effects in a mouse model of MJD. Depending on the concentration, lithium has well-established collateral effects. At least, in mice, these side effects may be the result of differences in the ability of some individual mice to clear LiCl from the plasma. In humans, at a dose of 1.5 mEq/L the side effects are considered mild, but anorexia [83], tremors [84], nausea, diarrhea, vertigo,

confusion (American Psychiatric Association 2002), and cognitive impairment can occur [85]. Of relevance to this pathology, irreversible cerebellar toxicity due to lithium intoxication has long been recognized and can lead to ataxia, nystagmus, and dysarthria [86]. The pathophysiology of lithium-related ataxia appears to be related with loss of Purkinje cells in the cerebellum, with sparing of the surrounding basket cells [87]. Clinicians are aware of these risks and monitor lithium plasma levels of the patients' closely. Side effects need to be carefully analyzed since lithium can cause cerebellar toxicity even at so-called therapeutic levels [88].

While completing the experiments for this article, a human clinical trial with lithium carbonate was performed in MJD patients (<http://clinicaltrials.gov/ct2/show/record/NCT01096082>). This study demonstrated that lithium (at a dose of 0.5–0.8 mEq/L) was safe and well tolerated by patients during the trial period, but the disease progression was not improved after 48 weeks of follow-up, given by the Neurological Examination Score for the Assessment of Spinocerebellar Ataxia (NESSCA) and the Scale for the Assessment and Rating of Ataxia (SARA) scales. However, the authors were able to show that the patients treated with lithium had a slightly slower progression concerning two quantitative ataxia assessment tools, the mean PATA rate and the Click Test, as well as in the spinocerebellar ataxia functional index (SCAFI) and composite cerebellar functional score (CCFS), when compared to patients receiving placebo. Considering this minor improvement in a few ataxia measures, the authors proposed that a larger number of patients should be enrolled in a new clinical trial to clarify these results [89]. Although the dosage used in our study is considerably lower than that used in the human study, and our treatment was initiated 1 week before symptom onset, this clinical trial is in accordance with the present study, where we could not find improvement by chronic LiCl treatment in the coordination and ataxia measurements, although some behavioral parameters, such as tremors and gait quality, were slightly ameliorated. Furthermore, we used similar doses as those administered in studies showing beneficial effects in mouse models of ALS and HD [44, 45] and confirmed that this dosage induced the expected biological effects, namely concerning autophagy induction.

AQ10

Conclusion

In conclusion, the present study, demonstrates that chronic lithium treatment is not able to rescue the CMVMJD135 mouse phenotype; our results do not

support lithium treatment as a good approach for MJD, particularly as the above mentioned side effects must be taken in consideration.

Acknowledgments

We would like to thank the animal caretaker Celina Barros for technical support. We thank Dr. Alexandra Estrada and Dra. Mónica Macedo from the Clinical and Pathological laboratory of Braga Hospital for the cooperation in the determination of plasma lithium levels. This work was supported by Fundação para a Ciência e Tecnologia through the projects [FEDER/FCT, POCI/SAU-MMO/60412/2004], and [PTDC/SAU-GMG/64076/2006]. This work was supported by Fundação para a Ciência e Tecnologia through fellowships [SFRH/BD/78388/2011 to S.D-S., SFRH/BPD/91562/2012 to A.S-F., SFRH/BD/51059/2010 to A.N-C., SFRH/BPD/79469/2011 to A.T-C.]. Sara Duarte-Silva states that she had full access to all of the data in the study and take responsibility for the integrity of the data and the accuracy of the data analysis.

Conflict of Interest

The authors do not report any conflict of interest.

Electronic supplementary material

Below is the link to the electronic supplementary material.

Supplementary figure 1

Levels of human ataxin-3 in LiCl-treated animals. Anti-ataxin-3 western-blot of brain lysates of transgenic animals injected with vehicle (veh) ($n = 4$) or lithium chloride (LiCl) 10.4 mg/Kg ($n = 4$) at 24 weeks of age. Actin was used as loading control. *, **, *** represents the $p < 0.05$; 0.01 or 0.001, respectively (test-t student). (GIF 14 kb)



High resolution image (TIFF 2617 kb)

Supplementary Table 1

Sample size calculations for each behavioral test assuming a power of 0.8 and a significance level of 0.05. (GIF 22 kb)



High resolution image (TIFF 2026 kb)

References

1. Lin D, Mok H, Yatham LN. Polytherapy in bipolar disorder. *CNS drugs*. 2006;20(1):29–42.
2. Goodwin FK. Rationale for using lithium in combination with other mood stabilizers in the management of bipolar disorder. *J Clin Psychiatr*. 2003;64 Suppl 5:18–24.
3. Gao XM, Fukamauchi F, Chuang DM. Long-term biphasic effects of lithium treatment on phospholipase C-coupled M3-muscarinic acetylcholine receptors in cultured cerebellar granule cells. *Neurochem Int*. 1993;22(4):395–403.
4. Ozaki N, Chuang DM. Lithium increases transcription factor binding to AP-1 and cyclic AMP-responsive element in cultured neurons and rat brain. *J Neurochem*. 1997;69(6):2336–44.
5. Klein PS, Melton DA. A molecular mechanism for the effect of lithium on development. *Proc Natl Acad Sci U S A*. 1996;93(16):8455–9.
6. Ryves WJ, Harwood AJ. Lithium inhibits glycogen synthase kinase-3 by competition for magnesium. *Biochem Biophys Res Commun*. 2001;280(3):720–5. doi: 10.1006/bbrc.2000.4169 .
7. Hashimoto R, Takei N, Shimazu K, Christ L, Lu B, Chuang DM. Lithium induces brain-derived neurotrophic factor and activates TrkB in rodent cortical neurons: an essential step for neuroprotection against glutamate excitotoxicity. *Neuropharmacology*. 2002;43(7):1173–9.
8. Fukumoto T, Morinobu S, Okamoto Y, Kagaya A, Yamawaki S. Chronic lithium treatment increases the expression of brain-derived neurotrophic factor in the rat brain. *Psychopharmacol (Berl)*. 2001;158(1):100–6. doi: 10.1007/s002130100871 .

9. Chen RW, Chuang DM. Long term lithium treatment suppresses p53 and Bax expression but increases Bcl-2 expression. A prominent role in neuroprotection against excitotoxicity. *J Biol Chem.* 1999;274(10):6039–42.
10. Hiroi T, Wei H, Hough C, Leeds P, Chuang DM. Protracted lithium treatment protects against the ER stress elicited by thapsigargin in rat PC12 cells: roles of intracellular calcium, GRP78 and Bcl-2. *Pharmacogenomics J.* 2005;5(2):102–11. doi: 10.1038/sj.tpj.6500296 .
11. Mattson MP, LaFerla FM, Chan SL, Leissring MA, Shepel PN, Geiger JD. Calcium signaling in the ER: its role in neuronal plasticity and neurodegenerative disorders. *Trends Neurosci.* 2000;23(5):222–9.
12. Bijur GN, De Sarno P, Jope RS. Glycogen synthase kinase-3beta facilitates staurosporine- and heat shock-induced apoptosis. Protection by lithium. *J Biol Chem.* 2000;275(11):7583–90.
13. Ren M, Senatorov VV, Chen RW, Chuang DM. Postinsult treatment with lithium reduces brain damage and facilitates neurological recovery in a rat ischemia/reperfusion model. *Proc Natl Acad Sci U S A.* 2003;100(10):6210–5. doi: 10.1073/pnas.0937423100 .
14. Wei H, Leeds PR, Qian Y, Wei W, Chen R, Chuang D. Beta-amyloid peptide-induced death of PC 12 cells and cerebellar granule cell neurons is inhibited by long-term lithium treatment. *Eur J Pharmacol.* 2000;392(3):117–23.
15. Rohn TT, Vyas V, Hernandez-Estrada T, Nichol KE, Christie LA, Head E. Lack of pathology in a triple transgenic mouse model of Alzheimer's disease after overexpression of the anti-apoptotic protein Bcl-2. *J Neurosci.* 2008;28(12):3051–9. doi: 10.1523/JNEUROSCI.5620-07.2008 .
16. Jacobsen JP, Mork A. The effect of escitalopram, desipramine, electroconvulsive seizures and lithium on brain-derived neurotrophic factor mRNA and protein expression in the rat brain and the correlation to 5-HT and 5-HIAA levels. *Brain Res.* 2004;1024(1–2):183–92. doi: 10.1016/j.brainres.2004.07.065 .
17. Berridge MJ, Downes CP, Hanley MR. Neural and developmental

actions of lithium: a unifying hypothesis. *Cell*. 1989;59(3):411–9.

18. Quiroz JA, Gould TD, Manji HK. Molecular effects of lithium. *Mol Interv*. 2004;4(5):259–72. doi: 10.1124/mi.4.5.6 .

19. Phiel CJ, Klein PS. Molecular targets of lithium action. *Annu Rev Pharmacol Toxicol*. 2001;41:789–813. doi: 10.1146/annurev.pharmtox.41.1.789 .

20. Sarkar S, Floto RA, Berger Z, Imarisio S, Cordenier A, Pasco M, et al. Lithium induces autophagy by inhibiting inositol monophosphatase. *J Cell Biol*. 2005;170(7):1101–11. doi: 10.1083/jcb.200504035 .

21. Sarkar S, Rubinsztein DC. Inositol and IP3 levels regulate autophagy: biology and therapeutic speculations. *Autophagy*. 2006;2(2):132–4.

22. Melendez A, Hall DH, Hansen M. Monitoring the role of autophagy in *C. elegans* aging. *Methods Enzymol*. 2008;451:493–520. doi: 10.1016/S0076-6879(08)03229-1 .

23. Xu M, Zhang HL. Death and survival of neuronal and astrocytic cells in ischemic brain injury: a role of autophagy. *Acta Pharmacol Sin*. 2011;32(9):1089–99. doi: 10.1038/aps.2011.50 .

24. Rubinsztein DC. Autophagy induction rescues toxicity mediated by proteasome inhibition. *Neuron*. 2007;54(6):854–6. doi: 10.1016/j.neuron.2007.06.005 .

25. Rubinsztein DC, Gestwicki JE, Murphy LO, Klionsky DJ. Potential therapeutic applications of autophagy. *Nat Rev Drug Discov*. 2007;6(4):304–12. doi: 10.1038/nrd2272 .

26. Lee SJ, Lim HS, Masliah E, Lee HJ. Protein aggregate spreading in neurodegenerative diseases: problems and perspectives. *Neurosci Res*. 2011;70(4):339–48. doi: 10.1016/j.neures.2011.05.008 .

27. Levine B, Kroemer G. Autophagy in the pathogenesis of disease. *Cell*. 2008;132(1):27–42. doi: 10.1016/j.cell.2007.12.018 .

28. Cuervo AM, Stefanis L, Fredenburg R, Lansbury PT, Sulzer D.

Impaired degradation of mutant alpha-synuclein by chaperone-mediated autophagy. *Science*. 2004;305(5688):1292–5. doi: 10.1126/science.1101738 .

29. Cuervo AM. Autophagy: in sickness and in health. *Trends Cell Biol*. 2004;14(2):70–7. doi: 10.1016/j.tcb.2003.12.002 .

30. Ravikumar B, Vacher C, Berger Z, Davies JE, Luo S, Oroz LG, et al. Inhibition of mTOR induces autophagy and reduces toxicity of polyglutamine expansions in fly and mouse models of Huntington disease. *Nat Genet*. 2004;36(6):585–95. doi: 10.1038/ng1362 .

31. Sarkar S, Ravikumar B, Floto RA, Rubinsztein DC. Rapamycin and mTOR-independent autophagy inducers ameliorate toxicity of polyglutamine-expanded huntingtin and related proteinopathies. *Cell Death Differ*. 2009;16(1):46–56. doi: 10.1038/cdd.2008.110 .

32. Ravikumar B, Duden R, Rubinsztein DC. Aggregate-prone proteins with polyglutamine and polyalanine expansions are degraded by autophagy. *Hum Mol Genet*. 2002;11(9):1107–17.

33. Nixon RA, Wegiel J, Kumar A, Yu WH, Peterhoff C, Cataldo A, et al. Extensive involvement of autophagy in Alzheimer disease: an immunoelectron microscopy study. *J Neuropathol Exp Neurol*. 2005;64(2):113–22.

34. Webb JL, Ravikumar B, Atkins J, Skepper JN, Rubinsztein DC. Alpha-synuclein is degraded by both autophagy and the proteasome. *J Biol Chem*. 2003;278(27):25009–13. doi: 10.1074/jbc.M300227200 .

35. Berger Z, Ravikumar B, Menzies FM, Oroz LG, Underwood BR, Pangalos MN, et al. Rapamycin alleviates toxicity of different aggregate-prone proteins. *Hum Mol Genet*. 2006;15(3):433–42. doi: 10.1093/hmg/ddi458 .

36. Menzies FM, Huebener J, Renna M, Bonin M, Riess O, Rubinsztein DC. Autophagy induction reduces mutant ataxin-3 levels and toxicity in a mouse model of spinocerebellar ataxia type 3. *Brain : J Neurol*. 2010;133(Pt 1):93–104. doi: 10.1093/brain/awp292 .

37. Nascimento-Ferreira I, Santos-Ferreira T, Sousa-Ferreira L, Auregan

G, Onofre I, Alves S et al. Overexpression of the autophagic beclin-1 protein clears mutant ataxin-3 and alleviates Machado-Joseph disease. *Brain*. 2011. doi: 10.1093/brain/awr047 .

38. Meijer AJ, Codogno P. Regulation and role of autophagy in mammalian cells. *Int J Biochem Cell Biol*. 2004;36(12):2445–62. doi: 10.1016/j.biocel.2004.02.002 .

39. Yu WH, Cuervo AM, Kumar A, Peterhoff CM, Schmidt SD, Lee JH, et al. Macroautophagy—a novel beta-amyloid peptide-generating pathway activated in Alzheimer’s disease. *J Cell Biol*. 2005;171(1):87–98. doi: 10.1083/jcb.200505082 .

40. Menzies FM, Ravikumar B, Rubinsztein DC. Protective roles for induction of autophagy in multiple proteinopathies. *Autophagy*. 2006;2(3):224–5.

41. Xiong N, Jia M, Chen C, Xiong J, Zhang Z, Huang J, et al. Potential autophagy enhancers attenuate rotenone-induced toxicity in SH-SY5Y. *Neuroscience*. 2011;199:292–302. doi: 10.1016/j.neuroscience.2011.10.031 .

42. Stambolic V, Ruel L, Woodgett JR. Lithium inhibits glycogen synthase kinase-3 activity and mimics wingless signalling in intact cells. *Curr Biol*. 1996;6(12):1664–8.

43. Feng HL, Leng Y, Ma CH, Zhang J, Ren M, Chuang DM. Combined lithium and valproate treatment delays disease onset, reduces neurological deficits and prolongs survival in an amyotrophic lateral sclerosis mouse model. *Neuroscience*. 2008;155(3):567–72. doi: 10.1016/j.neuroscience.2008.06.040 .

44. Fornai F, Longone P, Cafaro L, Kastsuchenka O, Ferrucci M, Manca ML et al. Lithium delays progression of amyotrophic lateral sclerosis. *Proceedings of the National Academy of Sciences of the United States of America*. 2008;105(6):2052-7. doi: 10.1073/pnas.0708022105

45. Wood NI, Morton AJ. Chronic lithium chloride treatment has variable effects on motor behaviour and survival of mice transgenic for the Huntington’s disease mutation. *Brain Res Bull*. 2003;61(4):375–83.

46. Watase K, Gatchel JR, Sun Y, Emamian E, Atkinson R, Richman R, et al. Lithium therapy improves neurological function and hippocampal dendritic arborization in a spinocerebellar ataxia type 1 mouse model. *PLoS Med.* 2007;4(5):e182. doi: 10.1371/journal.pmed.0040182 .
47. Jia DD, Zhang L, Chen Z, Wang CR, Huang FZ, Duan RH et al. Lithium chloride alleviates neurodegeneration partly by inhibiting activity of GSK3beta in a SCA3 *Drosophila* model. *Cerebellum.* 2013. doi: 10.1007/s12311-013-0498-3 .
48. Silva-Fernandes A, Duarte-Silva S, Neves-Carvalho A, Amorim M, Soares-Cunha C, Oliveira P et al. Chronic treatment with 17-DMAG improves balance and coordination in a new mouse model of Machado-Joseph disease. *Neurotherapeutics : the journal of the American Society for Experimental NeuroTherapeutics.* 2014. doi: 10.1007/s13311-013-0255-9 .
49. Nicklas W, Baneux P, Boot R, Decelle T, Deeny AA, Fumanelli M, et al. Recommendations for the health monitoring of rodent and rabbit colonies in breeding and experimental units. *Lab Anim.* 2002;36(1):20–42.
50. Silva-Fernandes A, Costa MD, Duarte-Silva S, Oliveira P, Botelho CM, Martins L et al. Motor uncoordination and neuropathology in a transgenic mouse model of Machado-Joseph disease lacking intranuclear inclusions and ataxin-3 cleavage products. *Neurobiol Dis.* 2010. doi: 10.1016/j.nbd.2010.05.021 .
51. Rogers DC, Fisher EM, Brown SD, Peters J, Hunter AJ, Martin JE. Behavioral and functional analysis of mouse phenotype: SHIRPA, a proposed protocol for comprehensive phenotype assessment. *Mamm Genome : Off J Int Mamm Genome Soc.* 1997;8(10):711–3.
52. Carter RJ, Lione LA, Humby T, Mangiarini L, Mahal A, Bates GP, et al. Characterization of progressive motor deficits in mice transgenic for the human Huntington's disease mutation. *J Neurosci : Off J Soc Neurosci.* 1999;19(8):3248–57.
53. Rafael JA, Nitta Y, Peters J, Davies KE. Testing of SHIRPA, a mouse phenotypic assessment protocol, on Dmd(mdx) and Dmd(mdx3cv) dystrophin-deficient mice. *Mamm Genome.* 2000;11(9):725–8. doi: 10.1007/s003350010149 .

54. JH Z. Biostatistical analysis (4th Edition). Prentice Hall; 1999
55. Klionsky DJ, Abeliovich H, Agostinis P, Agrawal DK, Aliev G, Askew DS, et al. Guidelines for the use and interpretation of assays for monitoring autophagy in higher eukaryotes. *Autophagy*. 2008;4(2):151–75.
56. Itakura E, Kishi C, Inoue K, Mizushima N. Beclin 1 forms two distinct phosphatidylinositol 3-kinase complexes with mammalian Atg14 and UVRAG. *Mol Biol Cell*. 2008;19(12):5360–72. doi: 10.1091/mbc.E08-01-0080 .
57. Baptista T, Teneud L, Contreras Q, Alastre T, Burguera JL, de Burguera M, et al. Lithium and body weight gain. *Pharmacopsychiatry*. 1995;28(2):35–44. doi: 10.1055/s-2007-979586 .
58. Saute JAM, da Silva ACF, Souza GN, Russo AD, Donis KC, Vedolin L, et al. Body mass index is inversely correlated with the expanded CAG repeat length in SCA3/MJD patients. *Cerebellum*. 2012;11(3):771–4.
59. Lalonde R, Strazielle C. Brain regions and genes affecting limb-clasping responses. *Brain Res Rev*. 2011;67(1–2):252–9. doi: 10.1016/j.brainresrev.2011.02.005 .
60. Chou AH, Yeh TH, Ouyang P, Chen YL, Chen SY, Wang HL. Polyglutamine-expanded ataxin-3 causes cerebellar dysfunction of SCA3 transgenic mice by inducing transcriptional dysregulation. *Neurobiol Dis*. 2008;31(1):89–101. doi: 10.1016/j.nbd.2008.03.011 .
61. Cemal CK, Carroll CJ, Lawrence L, Lowrie MB, Ruddle P, Al-Mahdawi S, et al. YAC transgenic mice carrying pathological alleles of the MJD1 locus exhibit a mild and slowly progressive cerebellar deficit. *Hum Mol Genet*. 2002;11(9):1075–94.
62. Mangiarini L, Sathasivam K, Seller M, Cozens B, Harper A, Hetherington C, et al. Exon 1 of the HD gene with an expanded CAG repeat is sufficient to cause a progressive neurological phenotype in transgenic mice. *Cell*. 1996;87(3):493–506.
63. Fernagut PO, Diguët E, Bioulac B, Tison F. MPTP potentiates 3-nitropropionic acid-induced striatal damage in mice: reference to

striatonigral degeneration. *Exp Neurol*. 2004;185(1):47–62.

64. Wirths O, Weis J, Kayed R, Saido TC, Bayer TA. Age-dependent axonal degeneration in an Alzheimer mouse model. *Neurobiol Aging*. 2007;28(11):1689–99. doi: 10.1016/j.neurobiolaging.2006.07.021 .

65. Lalonde R, Dumont M, Staufenbiel M, Strazielle C. Neurobehavioral characterization of APP23 transgenic mice with the SHIRPA primary screen. *Behav Brain Res*. 2005;157(1):91–8. doi: 10.1016/j.bbr.2004.06.020 .

66. Lalonde R, Lewis TL, Strazielle C, Kim H, Fukuchi K. Transgenic mice expressing the betaAPP695SWE mutation: effects on exploratory activity, anxiety, and motor coordination. *Brain Res*. 2003;977(1):38–45.

67. Brooks SP, Dunnett SB. Tests to assess motor phenotype in mice: a user's guide. *Nat Rev Neurosci*. 2009;10(7):519–29. doi: 10.1038/nrn2652 .

68. Riess O, Rub U, Pastore A, Bauer P, Schols L. SCA3: neurological features, pathogenesis and animal models. *Cerebellum*. 2008;7(2):125–37. doi: 10.1007/s12311-008-0013-4 .

69. Costa MD, Paulson HL. Toward understanding Machado-Joseph disease. *Prog Neurobiol*. 2011. doi: 10.1016/j.pneurobio.2011.11.006

70. Matos CA, de Macedo-Ribeiro S, Carvalho AL. Polyglutamine diseases: the special case of ataxin-3 and Machado-Joseph disease. *Prog Neurobiol*. 2011;95(1):26–48. doi: 10.1016/j.pneurobio.2011.06.007 .

71. Xiao H, Tang J, Hu Z, Tan J, Tang B, Jiang Z. [Polyglutamine-expanded ataxin-3 is degraded by autophagy]. *Zhonghua Yi Xue Yi Chuan Xue Za Zhi*. 2010;27(1):23-8. doi: 10.3760/cma.j.issn.1003-9406.2010.01.005 .

72. Paulson HL, Perez MK, Trottier Y, Trojanowski JQ, Subramony SH, Das SS, et al. Intranuclear inclusions of expanded polyglutamine protein in spinocerebellar ataxia type 3. *Neuron*. 1997;19(2):333–44.

73. Cheung ZH, Ip NY. Autophagy deregulation in neurodegenerative

- diseases—recent advances and future perspectives. *J Neurochem.* 2011;118(3):317–25. doi: 10.1111/j.1471-4159.2011.07314.x .
74. Mizushima N, Levine B, Cuervo AM, Klionsky DJ. Autophagy fights disease through cellular self-digestion. *Nature.* 2008;451(7182):1069–75. doi: 10.1038/nature06639 .
75. Goti D, Katzen SM, Mez J, Kurtis N, Kiluk J, Ben-Haiem L, et al. A mutant ataxin-3 putative-cleavage fragment in brains of Machado-Joseph disease patients and transgenic mice is cytotoxic above a critical concentration. *J Neurosci : Off J Soc Neurosci.* 2004;24(45):10266–79. doi: 10.1523/JNEUROSCI.2734-04.2004 .
76. Schmitt I, Brattig T, Gossen M, Riess O. Characterization of the rat spinocerebellar ataxia type 3 gene. *Neurogenetics.* 1997;1(2):103–12.
77. Sanberg PR, Fibiger HC, Mark RF. Body weight and dietary factors in Huntington's disease patients compared with matched controls. *Med J Aust.* 1981;1(8):407–9.
78. Gelenberg AJ, Jefferson JW. Lithium tremor. *J Clin Psychiatry.* 1995;56(7):283–7.
79. Bettencourt C, Santos C, Coutinho P, Rizzu P, Vasconcelos J, Kay T, et al. Parkinsonian phenotype in Machado-Joseph disease (MJD/SCA3): a two-case report. *BMC Neurol.* 2011;11:131. doi: 10.1186/1471-2377-11-131 .
80. Coutinho P, Sequeiros J. Clinical, genetic and pathological aspects of Machado-Joseph disease. *J Genet Hum.* 1981;29(3):203–9.
81. Ishida C, Sakajiri K, Yoshikawa H, Sakashita Y, Okino S, Yamaguchi K, et al. Lower limb tremor in Machado-Joseph disease. *Neurology.* 1998;51(4):1225–6.
82. Nandagopal R, Moorthy SG. Dramatic levodopa responsiveness of dystonia in a sporadic case of spinocerebellar ataxia type 3. *Postgrad Med J.* 2004;80(944):363–5.
83. Savvopoulos S, Golaz J, Bouras C, Constantinidis J, Tissot R.

Huntington chorea. Anatomoclinical and genetic study of 17 cases. *Encéphale*. 1990;16(4):251–9.

84. Miodownik C, Witztum E, Lerner V. Lithium-induced tremor treated with vitamin B6: a preliminary case series. *Int J Psychiatry Med*. 2002;32(1):103–8.

85. Tremont G, Stern RA. Minimizing the cognitive effects of lithium therapy and electroconvulsive therapy using thyroid hormone. *Int J Neuropsychopharmacol*. 2000;3(2):175–86. doi: 10.1017/S1461145700001838 .

86. Grignon S, Bruguerolle B. Cerebellar lithium toxicity: a review of recent literature and tentative pathophysiology. *Thérapie*. 1996;51(2):101–6.

87. Peiffer J. Clinical and neuropathological aspects of long-term damage to the central nervous system after lithium medication. *Arch Psychiatr Nervenkr*. 1981;231(1):41–60.

88. Niethammer M, Ford B. Permanent lithium-induced cerebellar toxicity: three cases and review of literature. *Mov Disord*. 2007;22(4):570–3. doi: 10.1002/mds.21318 .

89. Saute JA, Machado de Castilhos R, Monte TL, Schumacher-Schuh AF, Donis KC, D'Avila R et al. A randomized, phase 2 clinical trial of lithium carbonate in Machado-Joseph disease. *Movement disorders : official journal of the Movement Disorder Society*. 2014. doi: 10.1002/mds.25803 .